

STATUS REPORT OF THE SHORT-PULSE FACILITY AT THE DELTA STORAGE RING*

A. Schick[#], M. Höner, H. Huck, M. Huck, S. Khan, R. Molo, P. Ungelenk
Center for Synchrotron Radiation (DELTA), TU Dortmund University, 44221 Dortmund, Germany

Abstract

At DELTA, a 1.5-GeV synchrotron light source operated by the TU Dortmund University, a short-pulse facility employing the CHG (Coherent Harmonic Generation) principle is in operation. Here, the interaction of an intense, ultrashort laser pulse and electrons in an undulator leads to microbunching of a small fraction of the electrons in the bunch. As a consequence, ultrashort, coherent synchrotron radiation pulses in the VUV regime are emitted at harmonics of the incident laser wavelength. In addition, coherent THz pulses on the sub-ps timescale are generated. In this paper, the latest improvements of the facility and recent measurements are presented, including investigation of the transverse coherence and detection of the CHG radiation using photoemission spectroscopy in a VUV beamline.

INTRODUCTION

Pump-probe experiments allow to study phenomena on the timescale of the duration of the pulses used to excite (“pump”) a sample and to analyze (“probe”) it. Ultrashort (< 100 fs) laser pulses with a wavelength in the near-infrared regime are readily available from Titanium:sapphire laser systems. However, reducing the wavelength of the probe pulse is desirable for many applications.

Synchrotron light sources cover a large part of the electromagnetic spectrum, from the THz to the hard x-ray regime, but the pulse duration is of the order of 30 - 100 ps [1]. Lowering the momentum-compaction factor allows to decrease the pulse length to a few picoseconds, but at a reduced beam current [2].

Accessing the sub-ps regime with conventional synchrotron light sources is possible by using the interaction of ultrashort near-infrared laser pulses with electrons in the storage ring. The femtoslicing method is already in routine operation for several years [3-5], making use of a laser-induced energy modulation of the electrons in an undulator and a consecutive transverse displacement of the modulated electrons due to the dispersion in the following dipole magnet. Using an aperture, ultrashort pulses emitted by a subsequent undulator are extracted at variable photon energies up to the x-ray regime. The drawback of this method is a very low photon rate, because only a very small part of the electron bunch contributes.

* Work supported by DFG INST 212/236-1 FUGG, BMBF and by the Federal State NRW.

[#] andreas.schick@tu-dortmund.de

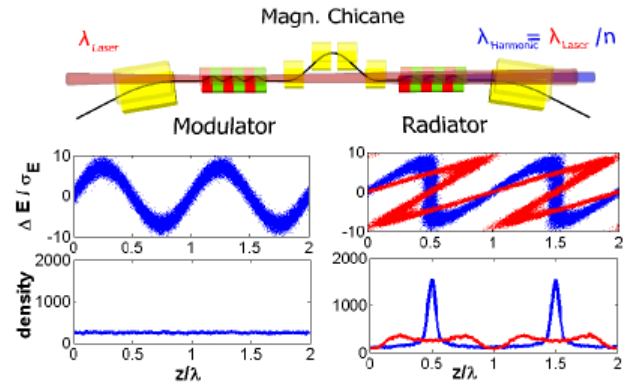


Figure 1: Sketch of an optical klystron (top). The electron energy is modulated sinusoidally (left) by a co-propagating laser pulse in the modulator. The microbunching caused by the magnetic chicane (right) leads to coherent emission of ultrashort synchrotron radiation pulses at harmonics of the laser wavelength in the radiator.

The Coherent Harmonic Generation (CHG) method also uses a laser-induced modulation of the electron energy, here imprinted in the first undulator (“modulator”) of an optical klystron, a configuration of two undulators, separated by a magnetic chicane, see Fig. 1. Due to energy-dependent path-length differences in the magnetic chicane, the sinusoidally modulated electron distribution is tilted, forming peaks in the electron density (“microbunching”). The degree of microbunching is described by the bunching factor b_n , which is given by [6]

$$|b_n| = e^{-\frac{1}{2}n^2B^2} J_n(nAB) \quad (1)$$

where n is the harmonic order, J_n is the Bessel function of the order n , $A = \Delta E/\sigma_E$ is the amplitude of the sinusoidal energy modulation in units of the natural energy spread σ_E and $B = R_{56} \cdot (2\pi/\lambda_{\text{Laser}}) \cdot (\sigma_E/E)$ is proportional to the transfer matrix element R_{56} of the chicane. The power of the CHG radiation emitted coherently at harmonics of the incident laser wavelength in the radiator scales with the bunching factor squared, which decreases exponentially with harmonic order [6]

$$P_{\text{coherent}}(\omega) \propto N_e^2 b_n^2 \propto e^{-n^2} \quad (2)$$

where N_e is the number of energy modulated electrons. Although only about 0.1 % of the whole electron bunch is modulated, the CHG radiation is 1-2 orders of magnitude more intense than the conventional synchrotron radiation emitted by the rest of the bunch, which only scales

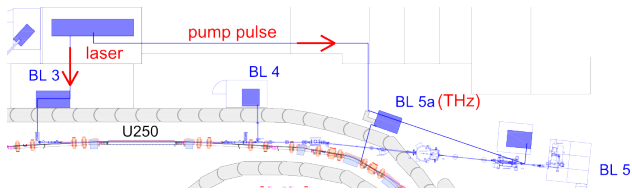


Figure 2: Sketch of the short-pulse facility at DELTA. Ultrashort laser pulses are transported and focused into the U250 undulator, operated as an optical klystron. CHG radiation can be detected at the beamlines BL 4 and BL 5, coherent THz radiation at beamline BL 5a.

linearly with the number of electrons. The CHG pulse duration is of the same order as that of the modulating laser pulse. Frequency doubling or tripling of the seed pulses enables the generation of even shorter wavelengths.

Besides CHG radiation, coherent and ultrashort THz pulses are generated by a sub-picosecond modulation of the electron density, which is caused by energy-dependent path-length differences in dipole magnets following the optical klystron.

SETUP

The short-pulse facility of DELTA, a 1.5 GeV synchrotron light source operated by the TU Dortmund University, is located in the northern part of the facility (see Fig. 2). The ultrashort pulses emitted by a commercial Titanium:sapphire laser system are frequency-doubled, corresponding to a laser wavelength of 400 nm, and transported into the undulator U250 by the beamline BL 3. The electromagnetic undulator is configured as an optical klystron with independently tunable modulator, chicane and radiator. The CHG radiation is either reflected into BL 4, where the laser-electron overlap is optimized and characterization measurements are performed, or into the photoelectron spectroscopy beamline BL 5. The beamline BL 4 is currently operated in air, preventing detection of radiation below 200 nm. An evacuated beamline is under construction.

Coherent ultrashort THz pulses at BL 5a are routinely used to detect and optimize the laser-electron overlap. Furthermore, pump-probe experiments in the THz regime will be performed in the future.

IMPROVEMENTS

Recently, the wiring of the chicane magnets in the optical klystron was changed, increasing the available chicane strength by about a factor of 10. Figure 3 shows the magnetic field of the old and new configuration (top) and the R_{56} value accumulated along the longitudinal position. Further details of the changes in the chicane configuration are explained in [7].

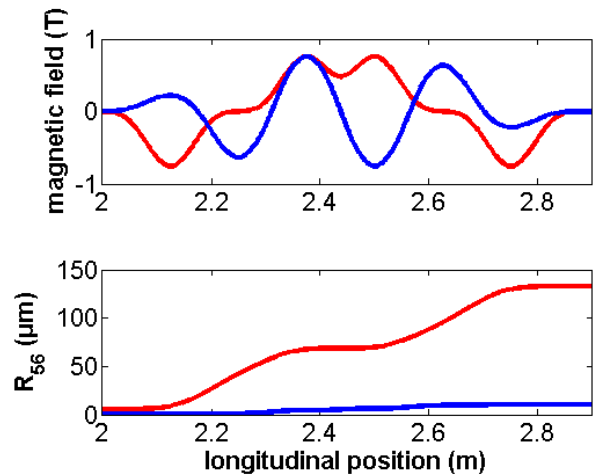


Figure 3: Magnetic field (top) and accumulated R_{56} value (bottom) of the old (blue) and new (red) chicane configuration as function of the longitudinal position.

The chicane strength available with the new configuration was deduced from the spectrum of the optical klystron radiation. The R_{56} value depends on the period of the spectral modulation induced by the arrival time difference of the light emitted by modulator and radiator, caused by the chicane (see Fig. 4) [8]. The R_{56} value was determined by fitting the measured spectra at different chicane currents.

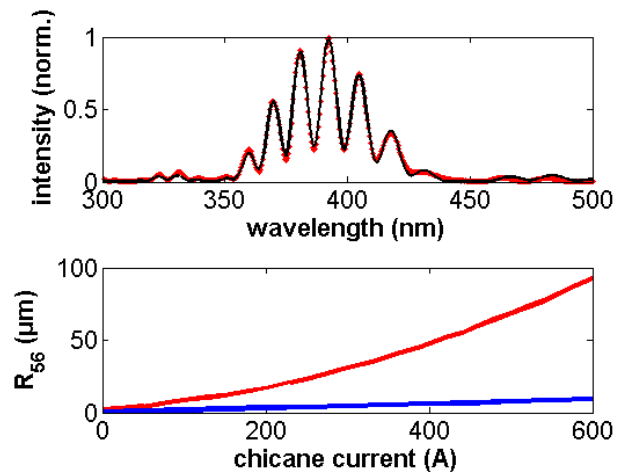


Figure 4: Top: measured (red) and fitted (black) optical klystron spectrum. Bottom: R_{56} value of the old (blue) and new (red) configuration, determined by fitting the optical klystron spectra as function of the chicane current.

The laser beamline, which transports the pump pulse from the laser system directly to BL 5a and BL 5 is evacuated and ready for operation.

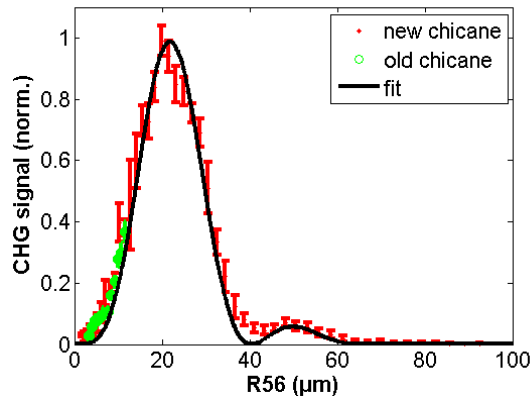


Figure 5: Measured (red) and fitted (black) CHG radiation as function of R_{56} value in the new and old (green) chicane configuration.

A delay stage, beam pointing stabilization and focusing of the laser beam have been set up in a dedicated, air-conditioned hutch at BL 5. The beam was focused on the sample and the zero delay between pump and probe pulse was found by a cross-correlation measurement using the two-photon absorption signal of a SiC photodiode.

LATEST RESULTS

The CHG signal was measured as function of the chicane strength (Fig. 5). Equation (1) was used to fit the acquired data and to determine the energy modulation amplitude A , which was 4.7 in this case. Previously, the optimum bunching factor, which is given by the maximum of the Bessel function (Eq. 1) could not be reached due to the limitation of the R_{56} value to approximately 11 μm .

Transverse Coherence

The transverse coherence of the CHG radiation was investigated by double-slit experiments. A fast-gated CCD camera [9] was used for the detection, since the repetition rate of the CHG radiation given by the laser is only 1 kHz, whereas the revolution frequency of the DELTA storage ring is 2.6 MHz. Without gating, integrating over many revolutions would result in excessive background of incoherent radiation.

Figure 6 shows the interference pattern of CHG (top) and incoherent radiation (bottom). The visibility of the fringes in the CHG pattern is 0.76, which is about a factor of 2 above that of the incoherent radiation. The factor would be even larger without the bandpass filter employed for the measurement.

Photoelectrons from CHG Radiation

One important step towards pump-probe operation of the short-pulse facility was the detection of CHG radiation in BL 5 by photoelectron emission on a gold sample. The beamline is equipped with a delay-line detector, which enables time-resolved detection of photoelectrons [10].

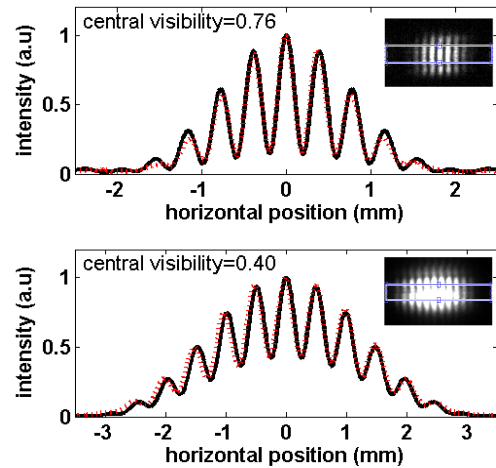


Figure 6: Measured (red) and fitted (black) interference pattern of the CHG (top) and incoherent (bottom) radiation approximately 1 m behind a double slit, both filtered with 10 nm FWHM bandpass filter.

The time resolution is determined by the time-of-flight distribution of the photoelectrons, which is of the order of several 10 ns. Figure 7 shows the photoelectron signal of 3 consecutive revolutions of a single bunch for the second and third harmonic. The signal at time zero contains incoherent and coherent radiation. The CHG radiation at the second harmonic is about 600 times and the third harmonic about 150 times brighter than the incoherent synchrotron radiation. A LiF filter with a cut-off wavelength of 120 nm was used to suppress higher diffraction orders of the monochromator. Furthermore, the fourth and fifth harmonic were observed, but with an increased incoherent radiation background since the LiF filter was removed.

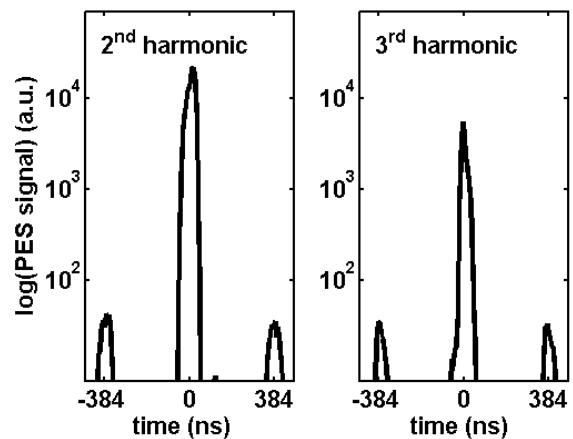


Figure 7: Photoelectron signal of three revolutions of a single bunch at the second and third harmonic, detected in BL 5. The signal at time zero is more intense due to the CHG contributions [10].

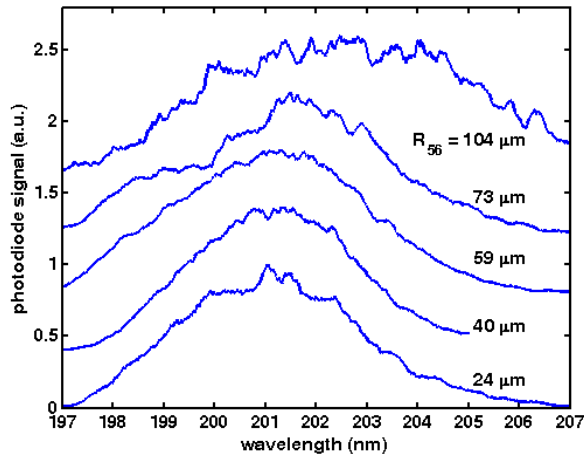


Figure 8: Spectra of second-harmonic CHG radiation measured under variation of the transfer matrix element R_{56} of the chicane. The spectra are normalized to a peak value of one and shifted vertically for clarity.

CHG Spectra as Function of the R_{56} Value

The energy modulation amplitude A is often assumed to be constant (e.g. [6]), but in reality it follows the electric field distribution of the seed laser pulse. Optimum microbunching is only obtained for particular values of A in a region at the center of the laser pulse or on its slopes, depending on the chicane setting. Spectra of CHG radiation should reflect the longitudinal distribution of the bunching factor and were measured for the second harmonic of a 400-nm seed under variation of the chicane strength, as shown in Fig. 8. Starting from an optimum value of $R_{56} = 40 \mu\text{m}$, the integrated intensity decreases and the spectral width increases when the chicane strength is reduced or increased.

Coherent THz Pulses

The THz beamline was equipped with a Fourier-transform spectrometer (FT-IR), enabling the spectrally resolved measurements described below.

THz spectra acquired with the FT-IR spectrometer are shown in Fig. 9. From a bending magnet, the far-infrared spectrum of conventional synchrotron radiation (blue) is expected to be almost constant. The shape shown here is related to the transfer function of the instrument, which is determined by the beamsplitter in the spectrometer for the lower cut-off. The suppression of higher frequencies is related to the z-cut quartz windows in the beamline. The spectrum acquired with laser-electron overlap (red) lies well within the transmission range of the beamline.

From the spectral distributions with and without overlap, the form factor $g(\nu)$ for the coherent synchrotron radiation [1] can be calculated. An inverse Fourier transform allows to estimate the longitudinal electron distribution induced by the laser-electron interaction. A fit of the form factor delivers values similar to previous simulations [11].

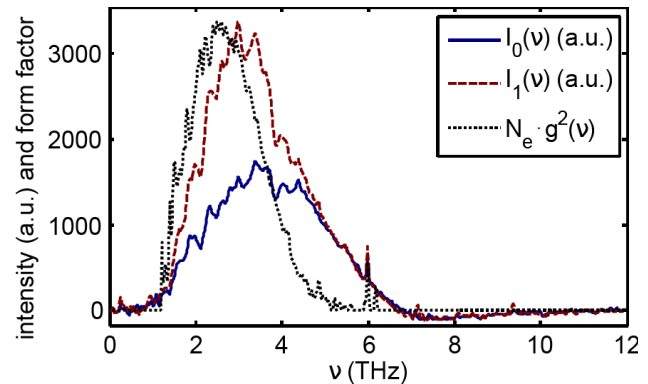


Figure 9: THz spectra detected with the FT-IR spectrometer with (red) and without (blue) laser-electron overlap.

Furthermore, observations of the THz radiation over several turns in the storage ring were performed using fast THz detectors. Coherent contributions in the THz pulses were detected up to the eighth turn after the laser-electron interaction [11].

OUTLOOK

The short-pulse facility at DELTA is in operation and under continuous improvement. First pump-probe experiments are planned towards the end of this year. In addition, an upgrade of BL 4 is planned, which enables the detection of CHG radiation down to 120 nm. The next step in reducing the CHG wavelength is to start seeding at the third harmonic of the Ti:Sapphire laser and to perform experiments at the fifth harmonic ($53 \text{ nm} \approx 23 \text{ eV}$) thereof.

ACKNOWLEDGMENT

It is a pleasure to thank our colleagues at DELTA and at the Forschungszentrum Jülich, as well as the technical staff of the Faculty of Physics for their continuous support. The project has profited from the expertise of our colleagues at many other labs, in particular HZB, MLS, DESY, KIT and SLS.

REFERENCES

- [1] H. Wiedemann, *Particle accelerator physics*, Springer (2007).
- [2] M. Abo-Bakr et al., PRL 90, 094801 (2003).
- [3] S. Khan et al., PRL 97, 074801 (2006).
- [4] R.W. Schoenlein et al., Science 287, 2237 (2000).
- [5] P. Beaud et al., PRL 99, 174801 (2007).
- [6] G. Stupakov, Phys. Rev. Lett. 102, 074801 (2009).
- [7] R. Molo et al., Proc. IPAC 2013, Shanghai, 1889.
- [8] P. Elleaume, Le Journal de Physique Colloques 44.CL,333 (1983).
- [9] The camera was provided by B. Schmidt and S. Wunderlich, DESY, Hamburg.
- [10] S. Khan et al., Sync. Rad. News 26 (3), 25 (2013).
- [11] P. Ungelenk et al., Proc. IPAC 2013, Shanghai, 94.